Deep Resources Engineering 1 (2024) 100112

Contents lists available at ScienceDirect

Deep Resources Engineering

journal homepage: www.keaipublishing.com/en/journals/deepre/

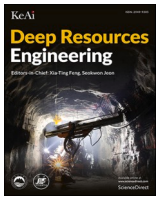

Full Length Article

Location method of ill-conditioned microseismic source and its engineering application

Bing-Rui Chen [a,b,*], Tao Li [c,d], Xinhao Zhu [c,d], Xu Wang [c,d], Qing Wang [c,d], Canxun Du [e], Sanlin Du [e]

[a] Key Laboratory of Ministry of Education on Safe Mining of Deep Metal Mines, Northeastern University, Shenyang 110819, China
[b] Key Laboratory of Liaoning Province on Deep Engineering and Intelligent Technology, Northeastern University, Shenyang 110819, China
[c] State Key Laboratory of Geomechanics and Geotechnical Engineering, Institute of Rock and Soil Mechanics, Chinese Academy of Sciences, Wuhan, Hubei 430071, China
[d] University of Chinese Academy of Sciences, Beijing 100049, China
[e] Huaneng Tibet Hydropower Safety Engineering Technology Research Center, Nyingchi, Tibet 860061, China

ARTICLE INFO

Keywords:
Microseismic
Location method
Ill-conditioned problem
Condition number singular value
Regularization
Newton downhill method

ABSTRACT

Microseismic event location is one of the core parameters in microseismic monitoring, and the accuracy of localization will directly affect the effectiveness of engineering applications. However, limited by spatial factors, the geometry of the sensor installation will be close to linear, which makes the localization equation suffer from the pathological problem, and the localization accuracy is greatly reduced. To address this problem, the reasons for the pathological problem are analyzed from the perspective of the objective function residuals and coefficient matrix. The pathological problem is caused by the combined effect of the poorer sensor array and data errors, and its residual isosurface shows a conical distribution, and as the residual value decreases, the apex of the isosurface gradually extends to the far side, and the localization results do not converge. For this reason, an improved regularized Newton downhill localization algorithm is proposed. In this method, firstly, the Newtonian downhill method is improved so that the magnitudes of the seismic source parameters are the same, and the condition number of the coefficient matrix is reduced; then, the L-curve method is used to calculate the regularization factor for the pathological equations, and the coefficient matrix is improved; finally, the pathological equations are regularized, and the seismic source coordinates are obtained by the improved Newtonian downhill method. The results of engineering applications show that compared with the traditional algorithm based on automatic of P-arrival picking, the number of effective microseismic events calculated by the proposed localization algorithm is increased by 194.7 %, and the localization accuracy is substantially improved. The proposed algorithm reduces the problem of low accuracy of S-arrival picking and allows localization using only P-wave arrival. The method reduces the quality requirements of the data and significantly improves the utilization of microseismic events and positioning accuracy.

1. Introduction

Microseismic monitoring has been widely used in mines, tunnels, hydropower stations, and hydraulic fracturing projects [7,13,25,29,30,41]. Source location is one of the key issues in research, whose result directly affects the calculation of source parameters, as well as the analysis of microseismic activity and disaster warning [23,43,44]. The accuracy of the positioning results largely determines the accuracy of the disaster warning. There are many factors that affect the accuracy of source location, such as sensor arrays, velocity models, and microseismic source location methods and et al. Researchers have conducted extensive studies in these areas. Kijko [16,17] and Mendecki [32] design a microseismic network based on D-optimality and C-optimality theory, respectively, and the two methods are mainly used to evaluate the merits and demerits of the sensor network. Chen et al. [3] propose a source location method based on a velocity model database and statistical analysis, providing effective technical support for mineral resources protection and mining safety. Peng et al. [33] consider the effect of the empty area on the microseismic event location and present a 3D heterogeneous velocity model for excavated tunnels, and its location

* Corresponding author at: Key Laboratory of Ministry of Education on Safe Mining of Deep Metal Mines, Northeastern University, Shenyang 110819, China.
E-mail address: brchen823@163.com (B.-R. Chen).

https://doi.org/10.1016/j.deepre.2024.100112
Received 19 May 2024; Received in revised form 20 July 2024; Accepted 25 August 2024
Available online 31 August 2024

accuracy is higher than that based on the single velocity model. Jiang et al. [15] propose a method for weighted STA/LTA (short-term average to long-term average) traces stacking for improving the location accuracy of the traditional stack-based method, and its location accuracy is higher than the traditional stack-based method and the arrival-based method. In recent years, seismic ray tracing theory has been introduced and computer technology has advanced, leading to the development of ray tracing and its related algorithms. Ray tracing can be categorized into two types: methods based on kinematic equations and methods based on grid cell extension [26,39]. The ray-tracing method can fully consider factors like airspace, viscoelasticity, and anisotropy. However, it is computationally intensive and less commonly used in practical engineering.

Currently, the location accuracy of common source location methods has been improved, and lies between 5 m and 50 m [4]. However, in the engineering site, such as mines, tunnels, shafts and *et al.*, due to the complex geological conditions, space limitations for construction operations, sensors can only be installed on one side of the target area. The distance from the installation section of the sensor array to the tunnelling face is approximately 70 m [14]. Simultaneously, to reduce the difficulty and cost of sensor installation, the drilling depth is set to be limited. Therefore, the size of the sensor array along the tunnel cross-section is limited. These factors contribute to the microseismic events occur outside the sensor array. In some cases, the sensors are even arranged close to a plane or a line. Under the function of monitoring data error, this approximate point-like and linear sensor arrangement will lead to the divergence of location results, resulting in ill-conditioned problems.

The numerical method of the source location includes the direct and iterative methods. The linear equations can be obtained through the Taylor series expansion of nonlinear problems. However, the stability and reliability of the solution will be further reduced when ill-conditioned problems occur. The source location can be attributed to the category of inverse problem mathematically, and the inverse problem is characterized by unsteadiness. Hansen [11] put forward the concept of ill-conditioned finite dimensional linear equations according to the characteristics of the solution of the least squares problem, and the coefficient matrix of the equations meets:(1) the condition number is very large; (2) the singular value gradually decreases and approaches zero. Therefore, ill-conditioned problems can be analyzed and solved according to these two characteristics.

Geiger method [8], Newton method [37], Joint location method [5], Powell method [34], and other methods [31] have been widely used in the source location; however, the ill-conditioned problems have not been studied. If all the rows or columns of the coefficient matrix have the same modulus, the condition number of the matrix will decrease and its ill-condition will be reduced [40]. Liu [27] proposed a new pre-processing method called two-side equalization method (TSEM), whose core idea is to reduce the condition number of coefficient matrices by equalizing the modules of matrix rows (columns). Ku [18] combined the pre-processing method with the dynamic Jacobian-inverse free method (DJIFM) to solve the ill-conditioned linear system with extreme physical contrast characteristics on the contact surface. Therefore, the pre-processing method [1] can reduce the condition number of the coefficient matrix, but it is difficult to achieve the expected effect for severely ill-conditioned linear equations. To further deal with ill-conditioned problems, many scholars have modified the singular value of the coefficient matrix to reduce its sensitivity to small disturbances in the inverse process and the condition number of the coefficient matrix, thus forming the ridge estimation method [42], truncated singular value decomposition method [2] and Tikhonov regularization method [28], among which Tikhonov regularization method is the most widely used. When the Tikhonov regularization method is used to solve the ill-conditioned problems, regularization factors will play a key role in inversion. If the regularization factor is excessively small, the condition number of the coefficient matrix does not improve and the approximate solution error is very large. However, if the regularization factor is excessively large, the solution of the constructed new problem is stable, which differs significantly from the original problem. When solving the regularization factors, the ridge trace method [19] is more intuitive, but its parameter selection has a certain degree of subjective arbitrariness. Generalized cross-validation (GCV) method [10] can theoretically select the optimal regularization factor, however, sometimes, the rate of change in GCV function is very slow. Comparatively, the L-curve method proposed by Hansen and Oleary [12] is a better method, wherein the point on the L-curve with the largest curvature corresponds to the position of the best regularization factor.

Therefore, aiming at the ill-conditioned problem in the source location, this paper obtains the variation trend of the condition number and singular values in the iterative process based on the improved Newton downhill (ND) method, and theoretically analyzes the causes of the ill-conditioned problems. To solve the ill-conditioned problem in localization, the ND method is improved and the regularization factor is introduced to weaken the influence of small singular value; therefore, a new improved source location method is proposed. Engineering verification shows that the proposed method solves the ill-conditioned problem caused by unreasonable sensor arrangement and improves the utilization rate of the monitoring data.

2. ill-conditioned problems and mechanism analysis

2.1. The ill-conditioned problems in source location

In source location, the objective function constructed in the sense of least squares is [8]

$$F(X) = (t_i - f_i(X))^2 \tag{1}$$

$$f_i(X) = \frac{\sqrt{(x_i - x_0)^2 + (y_i - y_0)^2 + (z_i - z_0)^2}}{v} + t_0 \tag{2}$$

where t_i indicates the observed arrival time of the i-th sensor, source parameters X=x_0, y_0, z_0, t_0; (x_0, y_0, z_0) are the source coordinates, and t_0 is the seismogenic time; $f_i(X)$ is the calculated arrival time of the i-th sensor. The nonlinear function $f_i(X)$ is expanded by the Taylor series in the neighborhood of the initial solution X^0, and the quadratic term is omitted. X^0 is equal to the coordinates and the monitoring arrival time of the first triggered sensor [24].

$$f_i(X) \approx f_i(X^0) + f_i'(X^0)\delta X \tag{3}$$

Where δX=$\{\delta x_0, \delta y_0, \delta z_0, \delta t_0\}^T$ is the source parameter correction. Let A=$f_i'(X^0)$, which is the partial derivative matrix. $b = t_i - f_i(X^0)$, which is the residual error vector. Therefore, the equation [8] becomes:

$$A\delta X = b \tag{4}$$

The coefficient matrix A is expressed as [8]

$$A = \begin{bmatrix} \frac{\partial f_1(X)}{\partial x_0} & \frac{\partial f_1(X)}{\partial y_0} & \frac{\partial f_1(X)}{\partial z_0} & 1 \\ \vdots & \vdots & \vdots & \vdots \\ \frac{\partial f_m(X)}{\partial x_0} & \frac{\partial f_m(X)}{\partial y_0} & \frac{\partial f_m(X)}{\partial z_0} & 1 \end{bmatrix} \tag{5}$$

To make the coefficient matrix a square matrix, let H=A^TA, B=A^Tb, then [8]

$$H\delta X = B \tag{6}$$

Where, the coefficient matrix $A \in R^{m\times 4}$, $H \in R^{4\times 4}$, and m is the number of the triggered sensors, m≥4.

According to the Hansen's definition of ill-conditioned problems, the coefficient matrix of the location equation needs to be solved to obtain

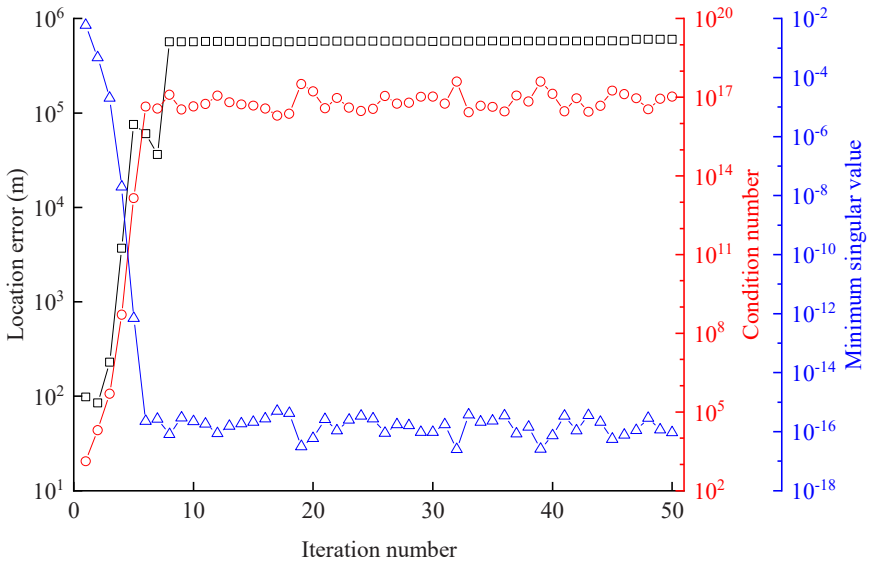

Fig. 1. Variation diagram of the location error, condition number, and minimum singular value of ill-conditioned event with iteration.

the condition number and singular value. The condition number of the coefficient matrix H [22] is

$$cond(H) = \left\|H^{-1}\right\| \cdot \|H\| \tag{7}$$

$cond(H)$ describes the sensitivity of the solution to the original data.

The iterative Equation of the ND method [24] can be expressed as

$$X^{n+1} = X^n - w(H^T H)^{-1} H^T B \tag{8}$$

X^n is the n-th iteration result of source parameters, and the value range of w is $0.5^{10} < w \leq 1$. To ensure convergence, w is required to make the objective function of each iteration meet [24].

$$F(X^{n+1}) < F(X^n) \tag{9}$$

The initial value of w is 1, and the value of w is halved each time the abovementioned Equation is not satisfied.

The singular value decomposition of matrix H [45] is

$$H = USV^T = \sum_{i=1}^{rank(H)} u_i \sigma_i v_i^T \tag{10}$$

where, the left matrix $U=(u_1, u_2, u_3, u_4)$, and $U=R^{4\times4}$, $UU^T=I$, which is the identity matrix. The right matrix $V=(v_1, v_2, v_3, v_4)$, $V=R^{4\times4}$, and $VV^T=I$. The diagonal matrix $S=\text{diag}(\sigma_1, \sigma_2, \sigma_3, \sigma_4)$ and the singular values σ_i are arranged in the decreasing order of $\sigma_1 \geq \sigma_2 \geq \sigma_3 \geq \sigma_4$.

In engineering practices, the sensor array in some engineering is adverse due to the limitation of sensor arrangement in space. Therefore, microseismic events can be easily triggered because of the ill-conditioned problems in localization. When the microseismic events are ill-conditioned, the ND method does not converge to the optimal solution after many iterations. Because the coefficient matrix is seriously ill-conditioned, the propagation and accumulation of errors make the location results far away from the optimal solution, which makes the iteration divergent. Consider an ill-conditioned event as an example, and its location error, condition number, and minimum singular with iteration are shown in Fig. 1. With the increase of iterative number, the condition number of the ill-conditioned event increases, and the minimum singular value decreases, and the location error increases gradually. When the iteration number reaches 8, the condition number, minimum singular value, and location result tend to be stable. Therefore, the frequent occurrence of ill-conditioned events in the monitoring will lead to divergence of location and deviation of energy calculation, thus disturbing the accuracy of rockburst prediction. Therefore, to solve the location problem of ill-conditioned events, it is necessary to study the characteristics of the ill-conditioned events.

Table 1
Sensors coordinates and arrival time of Event 1.

Sensor	Coordinates (m)			Arrival time (s)
	x	y	z	
A	0	0	0	0.24130
B	1000	0	0	0.10745
C	1000	1000	0	0.14423
D	0	1000	0	0.25977
E	0	0	1000	0.25189
F	1000	0	1000	0.12950
G	1000	1000	1000	0.16132
H	0	1000	1000	0.26964

2.2. Residual analysis

The essence of source location is to find the minimum residual point in the monitoring space, which is the position of micro-fracture. The difference between the observed arrival time and calculated arrival time from source to the sensor is represented by residual γ [32]:

$$\gamma = \sum_{i=1}^{n} (t_i - t_0 - t_{ci})^m \tag{11}$$

Let m=2, then the L2 norm is adopted for residual calculation. t_{ci} is the calculated arrival time of the i-th sensor.

Then, the estimated value of the seismogenic time t_0 is given as [21]

$$t_0 = \sum_{i=1}^{n} t_i/n - \sum_{i=1}^{n} t_{ci}/n \tag{12}$$

Substitute t_0 into Eq. (11), and the residual under the L2 norm criterion becomes [21]

$$\gamma = \sqrt{\sum_{i=1}^{n} \left[(t_i - \sum_{i=1}^{n} t_i/n) - (t_{ci} - \sum_{i=1}^{n} t_{ci}/n) \right]^2 / n} \tag{13}$$

From Eq. (13), it can be observed that residual γ is a function of spatial coordinates, and source coordinates can be obtained by solving the minimum value of residual in the spatial range.

To compare the residual effects of ill-conditioned and non-ill-conditioned events, two typical events are selected for comparison. Event 1 is the ideal data and a non-ill-conditioned event. As shown in Table 1, there is no error in the sensor coordinates and arrival time. The

Table 2
Sensors coordinates and arrival time of Event 2.

Sensor	Coordinates (m)			Arrival time (s)
	x	*y*	*z*	
301	6362.20	3895.60	935.53	6.02386
302	6363.80	3889.19	937.78	6.02311
303	6359.62	3903.97	935.64	6.02236
304	6354.22	3906.22	936.77	6.02161
305	6352.27	3898.39	937.38	6.02286

source location is (1206, 360, 421) (unit: m). Event 2 is an ill-conditioned event triggered by the shaft face of the Huize Lead-zinc Mine, and its sensor coordinates and arrival time are shown in Table 2. The position of the event is roughly estimated as (6360, 3900, 1046).

From Fig. 2, it can be observed that the residual isosurface of Event 1 presents an ellipsoid distribution. The ellipsoid decreases with the decrease in the residual value, and the ellipse finally shrinks to a point, whose coordinate is the source coordinates, and the location result of Event 1 converges. The residual distribution of Event 2 presents a conical distribution. As the residual value decreases, the vertices of the cone gradually extend to the distance, so the location result of Event 2 diverges. The residual isosurface of ill-conditioned events and non-ill-conditioned events are different, and the location results of ill-conditioned events diverge while those of non-ill-conditioned events converge.

2.3. Singular value analysis

To analyze the ill-conditioned problem, singular value decomposition (SVD) is applied to the coefficient matrix H. When there is an error in the monitoring data, B can be expressed as the sum of true value and error value, where $B=B_t+e$. B_t is the truth value and e is all types of error sets, including wave velocity and arrival time errors, etc. The decomposition of Eq. (6) can be obtained as [9]

$$\delta X = \sum_{i=1}^{rank(H)} \left(\frac{u_i^T * B_t}{\sigma_i} + \frac{u_i^T * e}{\sigma_i}\right) v_i \tag{14}$$

From Eq. (14), it can be observed that the pollution of the error value to the true solution is mainly reflected in the second term at the right end. When the singular value σ_i is abnormally small, the value of this error term is significantly large, even covering up the first term at the right end which reflects the true solution. As the iteration goes on, the errors spread and accumulate constantly, which will make the calculated solution farther away from the optimal solution, thus diverging the iteration. The coefficient matrix H is mainly related to the coordinates of the sensor array, and the singular value σ_i reflects the advantages and disadvantages of the sensor array. Therefore, to restrain the divergence of the iteration results, small singular values are required to be processed.

The studies of Rindorf [35] and Li et al. [20] show that when all the sensors are on a plane and not on a straight line, the source location will have two solutions, and the two solutions are symmetric about the plane. When all the sensors are in a straight line, the number of solutions is infinite, forming a circle perpendicular to the sensor line. When all the sensors are on the same hyperboloid, two solutions will be generated, which are on two focal points of the hyperboloid. For other sensor arrays, the source location can always converge to the true solution when there is no error in the data. The events may cause ill-conditioned problems when there are data errors in the monitoring system. Therefore, ill-conditioned events are caused by a combination of adverse sensor array and data errors. The sensor array generates interference location results by amplifying errors such as arrival time and wave velocity, thereby covering the true solution of the source location, and even causing location results to diverge. Simultaneously, the amplification degree of its location error is related to the ill-conditioned degree of the sensor array.

3. The improved regularized ND method

3.1. Improve ND method

The distance between the source and the i-th sensor is

$$\sqrt{(x_i - x_0)^2 + (y_i - y_0)^2 + (z_i - z_0)^2} = v(t_i - t_0) \tag{15}$$

To make the dimension of unknown parameters the same and the order of magnitude of parameter values at the same level, and thus reduce the condition number of the coefficient matrix, the above equation can be expressed as [4]

$$\sqrt{(x_i - x_0)^2 + (y_i - y_0)^2 + (z_i - z_0)^2} = r_i + r_0 \tag{16}$$

where $r_0=v(t_1-t_0)$, $r_i=v(t_i-t_1)$. t_1 is the arrival time of the earliest triggered sensor, and (x_0, y_0, z_0, r_0) is the unknown parameter.

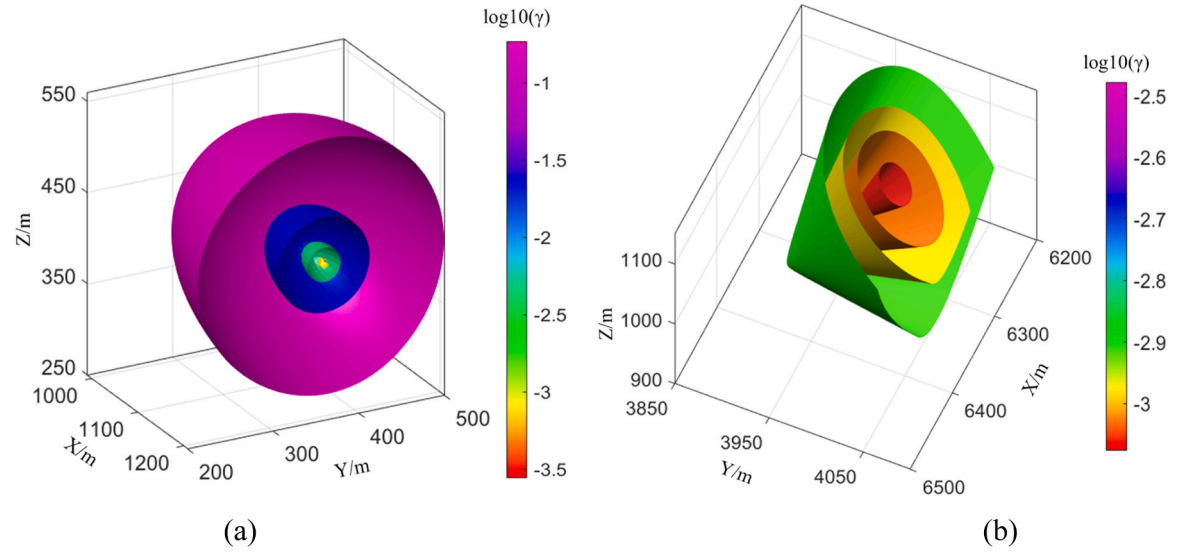

Fig. 2. Isosurface diagram of event residual. (a) Non-ill-conditioned event. (b) Ill-conditioned event.

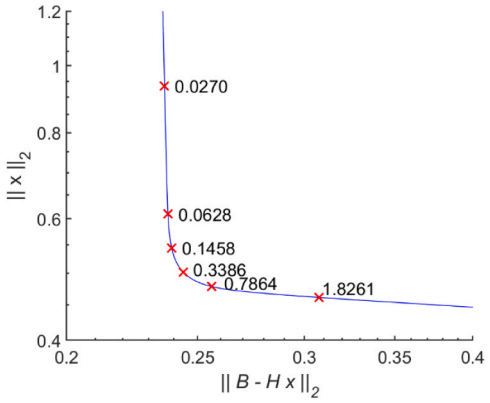

Fig. 3. L-curve.

$$f_i(X) = \sqrt{(x_i - x_0)^2 + (y_i - y_0)^2 + (z_i - z_0)^2} - r_0 - r_i \tag{17}$$

The partial derivative of the above equation to the parameter variables x_0, y_0, z_0, r_0 can be used to obtain the following linear equation.

$$A\delta X = b \tag{18}$$

where, the coefficient matrix $A \in R^{m\times 4}$. The expression of coefficient matrix A is

$$A = \begin{bmatrix} \frac{\partial f_1(X)}{\partial x_0} & \frac{\partial f_1(X)}{\partial y_0} & \frac{\partial f_1(X)}{\partial z_0} & -1 \\ \vdots & \vdots & \vdots & \vdots \\ \frac{\partial f_m(X)}{\partial x_0} & \frac{\partial f_m(X)}{\partial y_0} & \frac{\partial f_m(X)}{\partial z_0} & -1 \end{bmatrix} \tag{19}$$

The processes of Eq. (6)–(9) corresponding to the iterative process remain unchanged, and the source coordinates can be obtained by the ND method.

3.2. Regularization inversion

To better approximate the true solution, the regularization method is adopted to deal with the influence of small singular values, and the regularized objective function [6,38] in the sense of least squares is

$$\min[F(X) + \lambda F_m(X)] = \min(\|H\delta X - B\|_2^2 + \lambda \|C\delta X\|_2^2) \tag{20}$$

$$(H^T H + \lambda C^T C)\delta X = H^T B \tag{21}$$

$$(H^T H + \lambda C^T C)\delta X = H^T B \tag{21}$$

The expression of its solution vector is [11]

$$\delta X = \sum_{i=1}^{rank(H)} f_i \frac{u_i^T * B}{\sigma_i} v_i \tag{22}$$

where $F_m(X)$ is a stabilization functional, and C is a quasi-operator. f_i is the filter function and λ is the regularization factor or damping factor. When C is the identity matrix, the above equation is the standard Tikhonov regularization. Tikhonov regularization method weakens the matrix singularity by adding the regularization factor λ on the diagonal of the matrix, and its filter function f_i can be expressed as [11]

$$f_i = \frac{\sigma_i^2}{\sigma_i^2 + \lambda^2} \tag{23}$$

From the above equation, when $\sigma_i \gg \lambda$, filter function $f_i \approx 1$, and the regularization factor λ does not affect the singular value σ_i. When $\sigma_i \ll \lambda$, the filter function $f_i \approx 0$, the regularization factor λ completely suppresses the singular value. By changing the value of the regularization factor λ, the filter function f_i changes smoothly from 0 to 1. If reasonable regularization factors λ are given, small singular values can be suppressed.

3.3. Regularization inversion L-curve to solve the regularization factor λ

L-curve [12] takes $(\ln\|x_\lambda\|_2, \ln\|B - Hx_\lambda\|_2)$ as the point coordinate, Where $\|x_\lambda\|_2$ is the norm of regularization solution and $\|B - Hx_\lambda\|_2$ is the residual norm of regularization solution. For convenience, let $x_\lambda = \delta X$, L-curve in the rectangular coordinate system is shown in Fig. 3. Because the shape of the curve resembles the letter L, it is named L-curve. The optimal regularization parameters λ can be determined effectively by the L-curve, and the ill-conditioned problem can be transformed into a non-ill-conditioned problem. When the regularization factor λ is larger, it is equivalent to adding larger weight to the norm of the solution according to the Tikhonov regularization form; therefore, the norm of the regularization solution $\|x_\lambda\|_2$ becomes smaller and the residual norm of the regularization solution $\|B - Hx_\lambda\|_2$ becomes larger. In contrast, the residual norm of the regularization solution $\|B - Hx_\lambda\|_2$ becomes smaller when $\|x_\lambda\|_2$ becomes larger. From Fig. 3 shows that two quantities reach a good balance at the corner of the L-curve. Moreover, Hansen theoretically proved that the point at the "corner" is the optimal equilibrium point between the solution norm and the residual norm using the

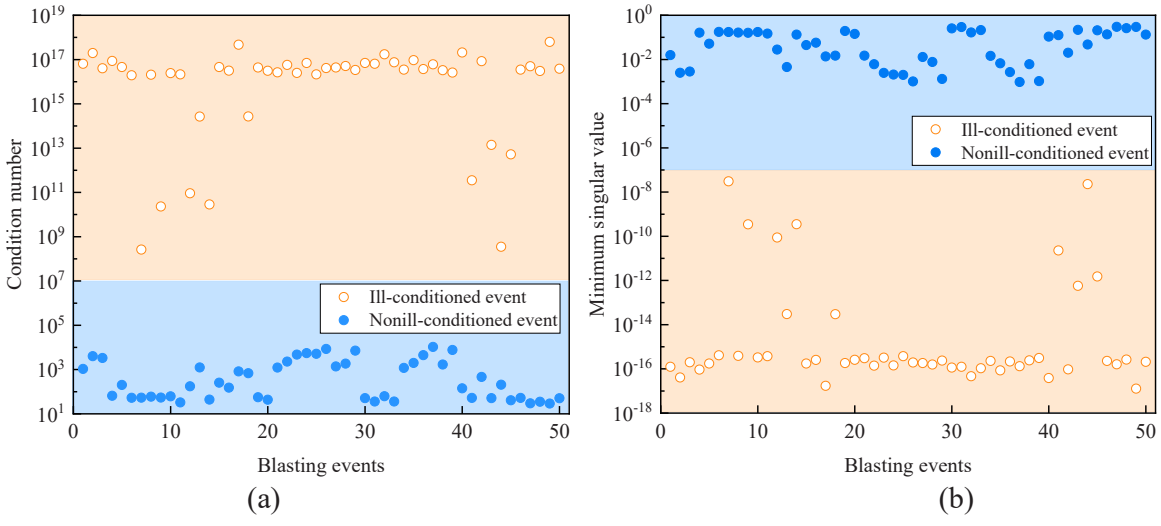

Fig. 4. Parameter comparison of ill-conditioned and non-ill-conditioned events. (a) Condition number. (b) Minimum singular value.

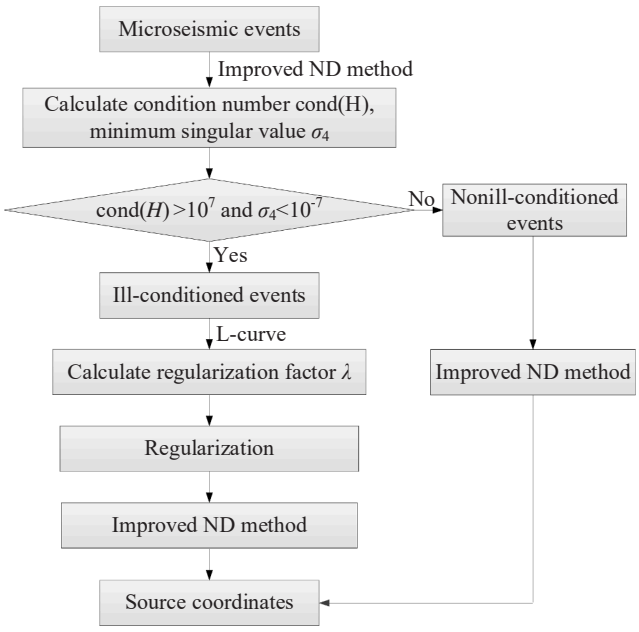

Fig. 5. Flowchart of improved regularized ND method.

singular value decomposition of matrix H and the curvature at this equilibrium point is the largest.

To calculate the curvature of the L-curve, first assume [12]

$$\eta = \|x_\lambda\|_2^2, \rho = \|B - Hx_\lambda\|_2^2 \tag{24}$$

The curvature [12] of the L-curve can be expressed as

$$k(\lambda) = 2\frac{\eta\rho}{\eta'}\frac{\lambda^2\eta'\rho + 2\lambda\eta\rho + \lambda^4\eta\eta'}{(\lambda^2\eta^2 + \rho^2)^{3/2}} \tag{25}$$

The regularization parameters λ at the point of maximum curvature can be calculated from the above equation.

3.4. Judgment of ill-conditioned events

Adding regularization processing in location calculation will increase the amount of calculation, so it is necessary to determine whether the events are ill-conditioned events before localization. To further analyze the characteristics of ill-conditioned events, 100 blasting events are randomly selected from an iron mine in Hebei province, including 50 ill-conditioned blasting events and 50 non-ill-conditioned blasting events. The minimum singular value and condition number at the end of the iteration are calculated by the improved ND method, as shown in Fig. 4.

From the comparison between the distribution of minimum singular value and condition number of ill-conditioned and non-ill-conditioned events, the critical value of the minimum singular value of ill-conditioned and non-ill-conditioned events is approximately 1.0×10^{-7}, and the critical value of the conditional number is approximately 1.0×10^7. The minimum singular values of non-ill-conditioned events are mainly concentrated in the range of $(1.0 \times 10^{-7}, 1)$, while the minimum singular values of ill-conditioned events are concentrated in the range of $(1.0 \times 10^{-18}, 1.0 \times 10^{-7})$. The condition number of the non-ill-conditioned events is mainly concentrated in the interval of $(10.0, 1.0 \times 10^7)$, while the condition number of ill-conditioned events is in the interval of $(1.0 \times 10^7, 1.0 \times 10^{19})$. Therefore, when the minimum singular value is less than 1.0×10^{-7} and the condition number is greater than 1.0×10^7 at the end of the iteration, the event is ill-conditioned.

3.5. Improved regularized ND method

To deal with the ill-conditioned problems in source location, an improved regularized ND method is proposed. The method first determines whether the event is ill-conditioned and then regularizes the ill-conditioned event. The flow chart is shown in Fig. 5, and the specific process is as follows:

(1) Input the arrival time of the triggering events and sensor coordinates.

(2) The condition number *cond*(*H*) and minimum singular value σ_4 of events are calculated by the improved ND method, and it is judged whether the condition number *cond*(*H*)>1.0×10^7 and minimum singular value σ_4< 1.0×10^{-7}.

(3) If the judgment conditions are not met, the event is non-ill-conditioned, and the improved ND method is used for localization to obtain the source coordinates. Otherwise, step (4) is performed.

(4) The event is judged to be ill-conditioned and the regularization factor λ is calculated by the L-curve.

(5) Eqs. (21) and (22) are used to regularize the equations in the iterative process of the improved ND method, and the solution vectors

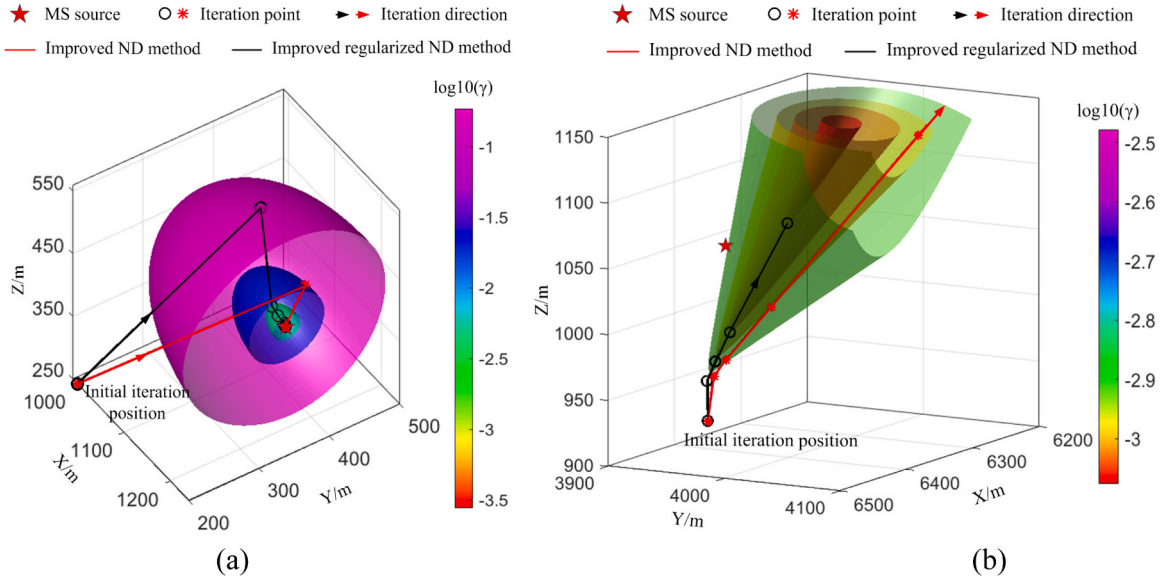

Fig. 6. Isosurface diagram of event residual and location iteration process. (a) Nonill-conditioned event. (b) Ill-conditioned event.

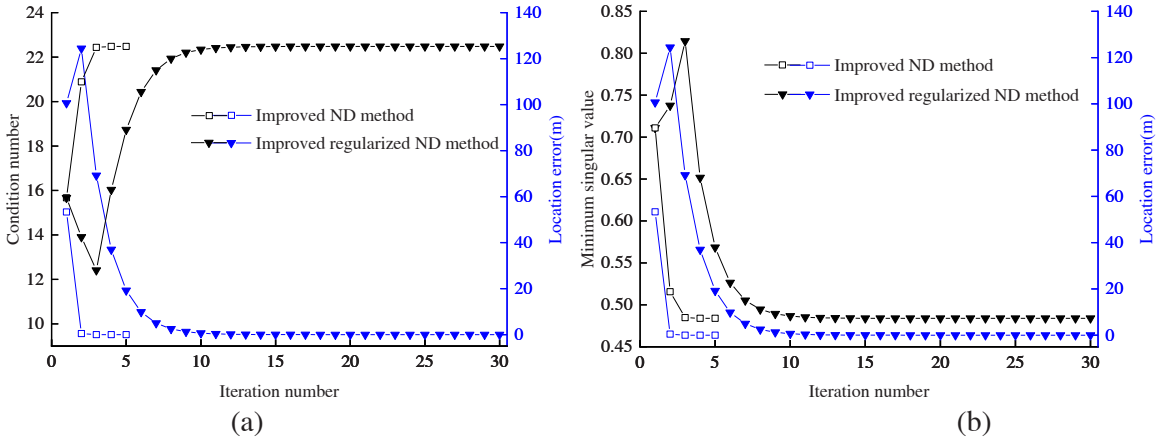

Fig. 7. Comparison of parameters of Event 1 in the iteration process. (a) Condition number. (b) Minimum singular value.

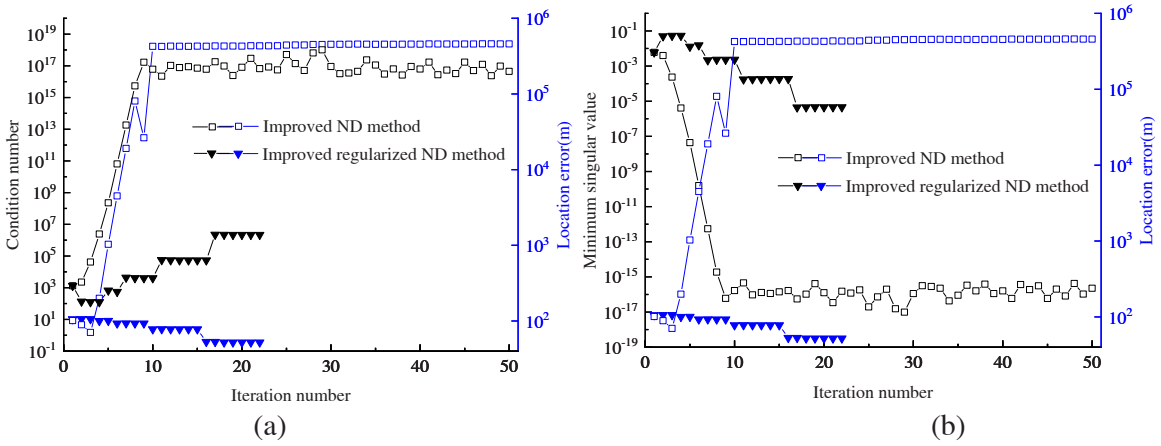

Fig. 8. Comparison of parameters of Event 2 in the iteration process. (a) Condition number. (b) Minimum singular value.

δX of each iteration are obtained.

(6) The solution vector of each iteration δX is taken as the new initial solution. The iteration ends and the source coordinates are obtained when the objective function meets the convergence allowable error.

4. Algorithm performance analysis

4.1. Performance analysis of improved ND method

To verify the improved effect of the ND method on condition number and singular value, the ND method and improved ND method are used to calculate the condition number and singular value of the two events in Tables 1 and 2, respectively. For Event 1, the condition number before improvement $cond(H)$=3.69 × 10^8, and the corresponding minimum singular value is 2.17 × 10^{-8}. The condition number after improvement $cond(H)$ =22.49 and the corresponding minimum singular value is 0.48. For Event 2, the conditions number before improvement $cond(H)$=6.41 × 10^{20}, and the corresponding minimum singular value is 7.80 × 10^{-20}. The improved condition number after the improvement $cond(H)$=6.31 × 10^{14}, and the corresponding minimum singular value is 1.58 × 10^{-16}. Compared to the ND method, the condition number of Events 1 and 2 is significantly reduced and the minimum singular value is significantly increased after the adoption of the improved ND method, which improves the ill-condition of the event. However, for ill-conditioned Event 2, the condition number is still large, the minimum singular value is still small, and the location result is divergent after adopting the improved ND method. Therefore, it is necessary to regularize the coefficient matrix after the improved ND method.

4.2. Performance analysis of improved regularized ND method

The improved ND method and the improved regularized ND method are used to locate the two events, and the residual isosurface and iteration process are shown in Fig. 6. For Event 1, both the methods converge well to the source coordinates, but the iterative steps of the improved regularized ND method increase. However, for Event 2, the location result of the improved ND method diverges towards the opening of the equivalent cone, while the improved regularized ND method converges to the adjacent region of the true solution. It can be seen that the location result of the improved ND method conforms to the residual evolution law, while the improved regularized ND method uses regularization to process data and eliminates the diffusion effect of the minimum singular value on the error, the location result converging.

Events 1 and 2 are located using the improved ND method and the improved regularized ND method. The evolution of condition number and minimum singular value in the iterative process are shown in Figs. 7 and 8 respectively. For Event 1, both the improved ND method and the improved regularized ND method can converge to the source position. However, the convergence rate of the improved ND method is faster than that of the improved regularized ND method. As the number of iterative steps increases, the minimum singular value and condition number of the two methods are at the same level. For Event 2, the location results diverge and the location error reaches more than 5.0 × 10^5 m when the improved ND method is used. With the increase of iteration steps, the minimum singular value gradually decreases to 1.0 × 10^{-19}, and the condition number increases to 1.0 × 10^{18}. In contrast, when the improved regularized ND method is adopted, the location

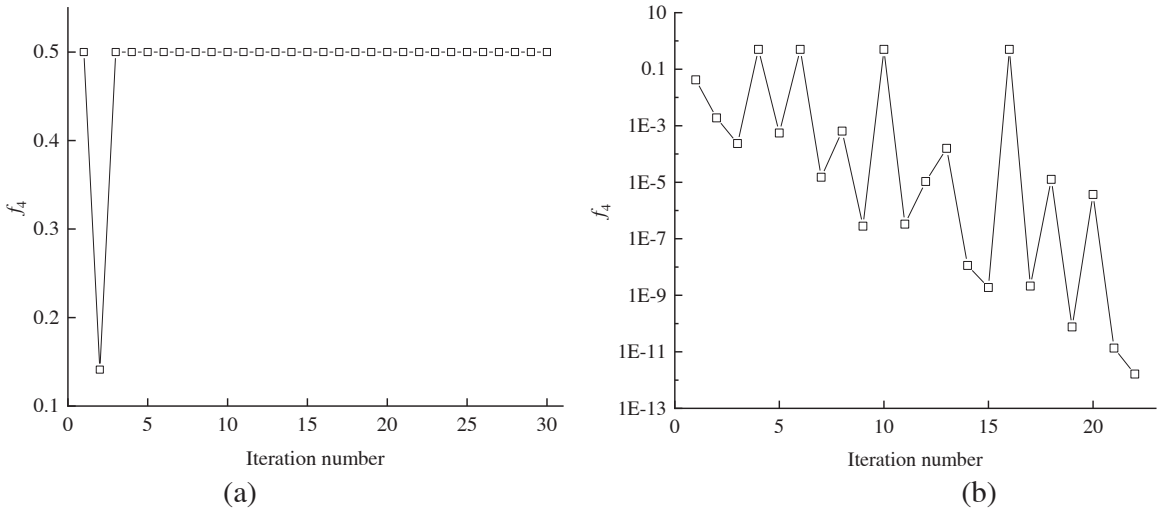

Fig. 9. Variation diagram of minimum filter function with iteration. (a) Nonill-conditioned event. (b) Ill-conditioned event.

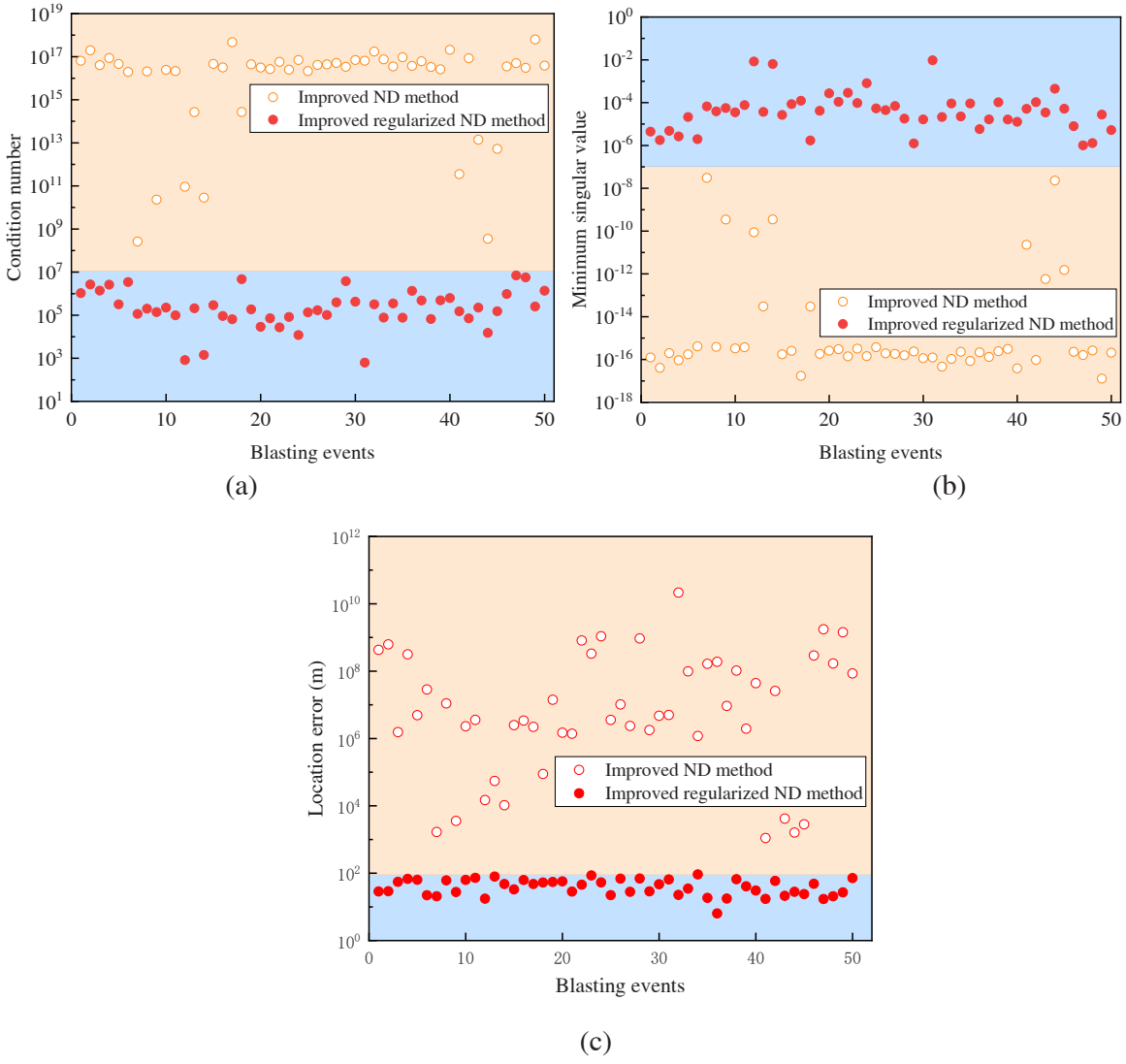

Fig. 10. Parameter comparison of ill-conditioned event. (a) Condition number. (b) Minimum singular value. (c) Location error.

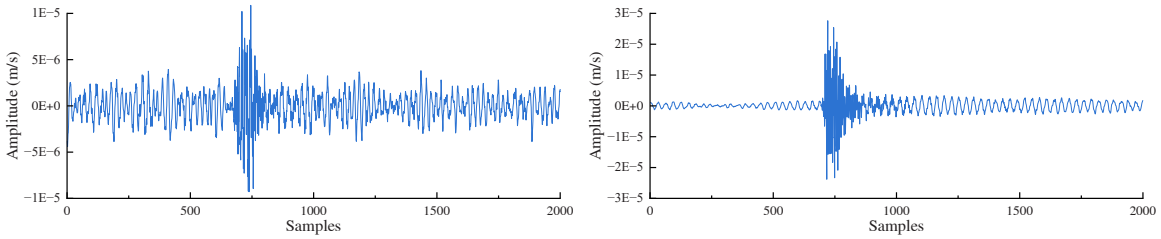

Fig. 11. Two typical microseismic signal in site.

results converge. With the increase of iteration steps, the minimum singular value decreases to approximately 1.0×10^{-5}, which is much larger than that of the improved ND method, and the condition number is controlled within 1.0×10^{7}, which is much smaller than that of the improved ND method.

According to the minimum singular value σ_4 and regularization factor λ of Events 1 and 2 in the iteration process, the minimum filter function f_4 is calculated by Eq. (23), and the variation of the minimum filter function with iteration is shown in Fig. 9. For Event 1, the minimum filter function f_4 gradually becomes stable with the increasing iteration steps, and its value is 0.5. Because of the existence of the filter function f_4, the correction value of each iteration is halved, which slows down the iteration; therefore, the improved regularized ND method has more iteration steps than the improved ND method. For Event 2, due to the influence of monitoring data error, with the increase of iteration, the minimum filter function gradually decreases from 0.5 to 0, thus eliminating the influence of singular value reduction.

For non-ill-conditioned events, there is a minimum residual value in space. Therefore, both the improved ND method and the improved regularized ND method can converge to the optimal position. However, compared with the improved ND method, the improved regularized ND method increases the amount of calculation, and the location effect is not improved. For ill-conditioned events, the residual error diverges in space, so the location result of the improved ND method diverges. Compared to the improved ND method, the location result of the improved regularization ND method converges, and the minimum singular value and condition number are reasonably controlled.

Furthermore, the improved regularized ND method is used to locate 50 ill-conditioned events in Fig. 4, and the minimum singular value, condition number and location error at the end of the iteration are calculated as shown in Fig. 10. For each of 50 ill-conditioned events, its condition number calculated by the improved regularized ND method is reduced below 1.0×10^{7}, its corresponding minimum singular value is increased above 1.0×10^{-7}, and its location error is mostly reduced to below 90 m. Through regularization processing, the condition number and the minimum singular value of the ill-conditioned event reach the nonill-conditioned range, and the ill-conditioned event improves significantly. Among the 50 adverse events, the proportion of location errors within 50 m is 64 % and the least location error is 7.8 m, which is a good location effect for some iron mine in Hebei province with many goafs.

5. Field test and application

To verify the reliability of the algorithm, microseismic monitoring data from a diversion tunnel was selected. This diversion tunnel is surrounded by granite rocks, and excavated by Tunnel Boring Machine (TBM). Under high ground stress, rockburst occurs near the tunnelling face frequently. To warn the rockburst disaster during the construction of a diversion tunnel and ensure the safety of tunnel construction, a SSS (SinoSeiSm) microseismic monitoring system, developed by Hubei Seaquake technology Co., Ltd., is hired for 24-hour uninterrupted monitoring of rock fracture and the schematic layout of sensors is shown in Fig. 11. Two groups of sensors are arranged along the axis direction of the diversion tunnel, and the sensors are arranged within the range of 140° of the tunnel top arch, and each group of sensors is located near the same cross-section. With the excavation of the tunnel, the sensor is repeatedly used following the movement of the tunnelling face; furthermore, the rock fracture signal near the tunnelling face can be obtained in real-time.

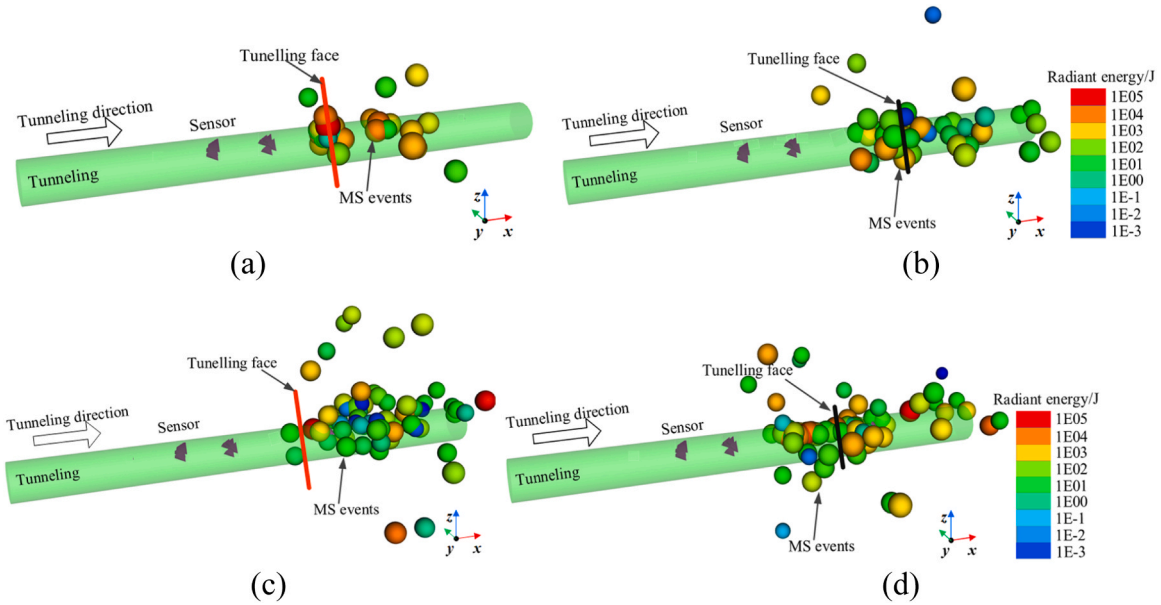

Fig. 12. Location results of rock fracture events from November 22 to November 24. (a) scheme No.1. (b) scheme No.2. (c) scheme No.3. (d) scheme No.4.

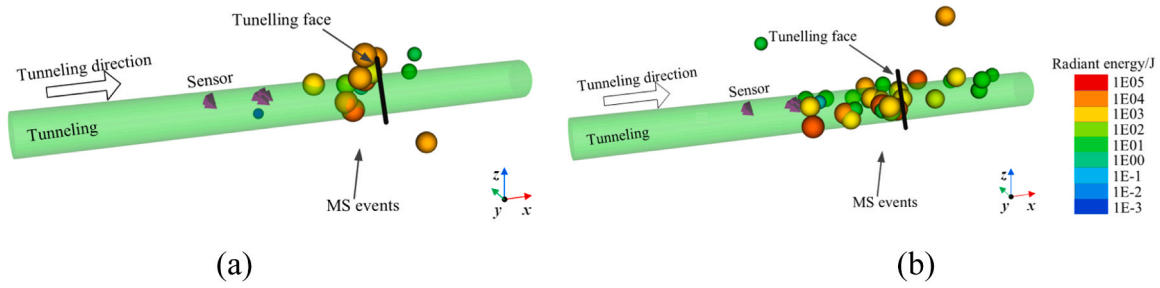

Fig. 13. Location results of rock fracture event from November 22 to November 24 based on (a) Geiger method and (b) PSO method.

Due to the numerous factors causing interference before and after the S-wave arrival, picking the S-wave arrival is more challenging compared to the P-wave. Hence, opting for only the P-wave arrival is a commonly employed method in location. However, because the number of sensors is few and the sensor array is not ideal in tunnelling engineering, especially excavated by TBM, it is easy to cause ill-conditioned problems only by using P-wave arrival for localization. Therefore, the proposed method is introduced to locate rock fracture source using only the arrival time of P-waves. To evaluate the effectiveness of the proposed method, we chose a set of microseismic events for testing, which were acquired by the SSS microseismic monitoring system over the period 22–24 November 2020. Some representative signals are displayed in Fig. 11, from which we can see that these signals have a low signal-to-noise ratio and it is difficult to accurately identify the S-wave arrival. These events are located by four different schemes. Scheme No.1 adopts P-wave arrival automatically picked up by the system and the ND method for localization; scheme No.2 adopts the P- and S-wave arrival, which is picked up automatically by the system and the ND method for localization; scheme No.3 adopts the P- and S-wave arrival, which is picked up manually and the ND method for localization; and scheme No.4 adopts P-wave arrival, which is picked up manually and the improved regularized ND method for localization.

The location results of the four schemes are shown in Fig. 12(a), (b), (c), and (d). The area range of the effective events is defined as: x direction is within the range of the first row of sensors to 20 m in front of the tunnelling face, and the cross-section ranges are $y\in$(-40 m, 40 m) and $z\in$(-40 m, 40 m). There are 38, 67, 69, and 112 effective events obtained by the four schemes respectively. Compared to scheme No.1, scheme No.2 adds S-wave arrival for location calculation, the number of the effective events increases by 76.3 %, and the number of non-ill-conditioned events increases significantly. The addition of S-wave arrival in the source location increases the information of the location equation and makes the location result more stable. Compared to Scheme No.2 and Scheme No.3, the number of the effective events, which are manually picked is more than those picked automatically, and the location results are more concentrated. It can be observed that picking P- and S-wave arrival manually improves the accuracy of location.

Compared to scheme No.1 and scheme No.3, the number of the effective events obtained by the proposed method increases by 194.7 % and 62.3 % respectively. The proposed method is optimal among the four schemes above, solves well the ill-conditioned problem of events, location of its events is concentrated 30 m behind and 10 m before the tunnelling face and is in accordance with the range of stress adjustment after the tunnelling face is excavated.

To further verify the superiority of the proposed method, the same rock fracture events, whose P-wave arrivals are picked up manually, are located by Geiger [8] and Particle Swarm Optimization (PSO) methods

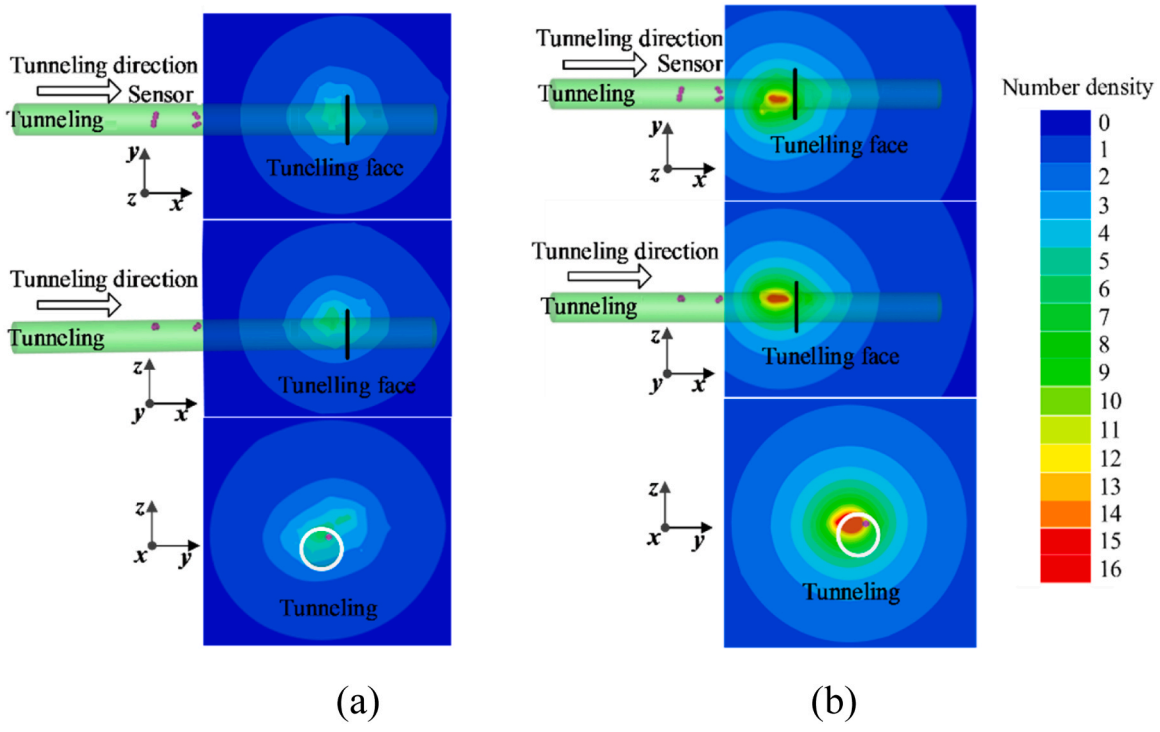

Fig. 14. Number density of rock fracture events from November 22 to November 24. (a) scheme No.3. (b) scheme No.4.

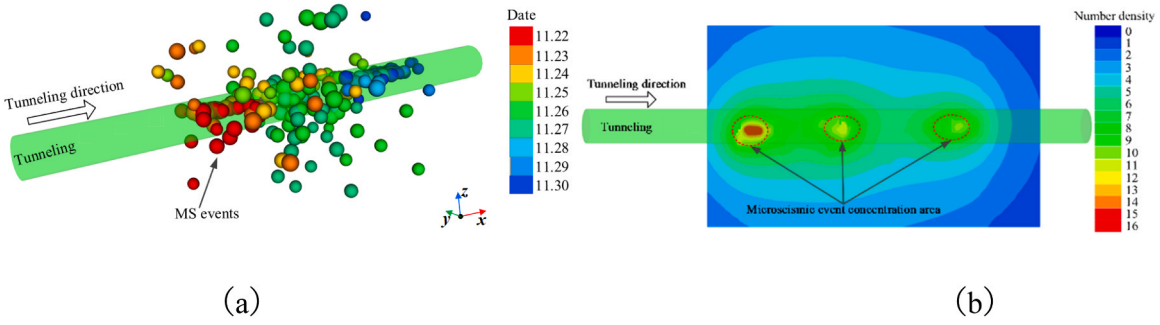

Fig. 15. Location of rock fracture event from November 22–30. (a) Variation of rock fracture event location with time. (b) Number density.

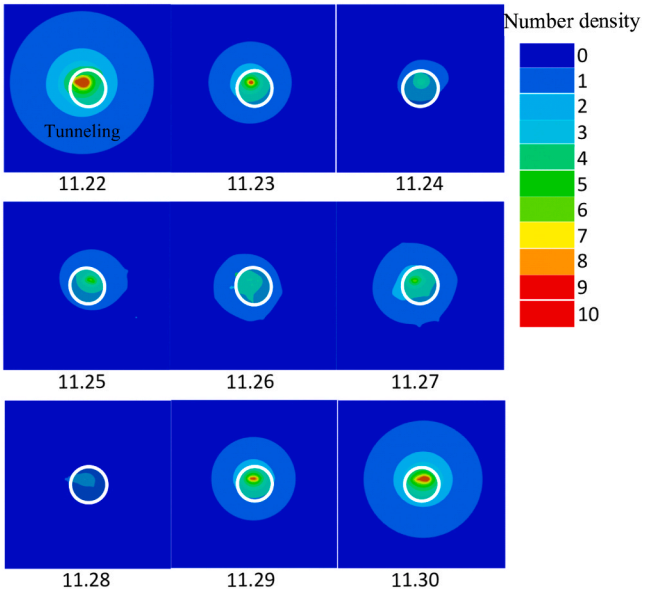

Fig. 16. Daily number density of rock fracture events from November 22–30.

[36], respectively. The location results are shown in Fig. 13(a) and (b), respectively. There are 18 and 34 effective events obtained by the Geiger and PSO methods, respectively. Comparing with these traditional methods, the new proposed method obtains more effective events and shows more concentrated trend. It shows that the new proposed method can better mine the microseismic information, reduce the divergence of arrival time, wave velocity, and other errors on localization, and improve the accuracy of source location. To further compare the location effects of scheme No.3 and scheme No.4, the number density of the effective events (the number of the effective events per unit volume, unit: m^3) is shown in Fig. 14 (a) and (b). From the comparison in Fig. 14 (a) and (b), the number density of the effective events obtained by scheme No.4 is larger than that of scheme No.3, and the location effect of the proposed method is more concentrated than that of the traditional method with richer arrival time information.

Compared to the traditional method, the improved regularized ND method requires less arrival time information; however, the location accuracy has been improved significantly. The proposed method avoids the problem of poor accuracy of S-wave picking and directly uses the automatically picked P-wave arrival to locate. This proposed method realizes the real-time localization and makes the data that can't be located effectively, thus improving the data quality and utilization rate. For monitoring scheme with limited sensor arrangement and adverse sensor array, the improved regularized ND method can improve the accuracy of the source location and increase the utilization rate of the signals, which has great application value.

Rock fracture events, monitored by the SSS microseismic monitoring system between the dates of 22–30 November 2020, are located by Scheme No.4, and the location result is shown in Fig. 15. The cross-sectional diagram of the daily number density of events changing with time is shown in Fig. 16. Over time, the rock fracture events gradually moved towards the direction of excavation, which in mainly concentrated in three areas. The concentration of rock microcracks are serious

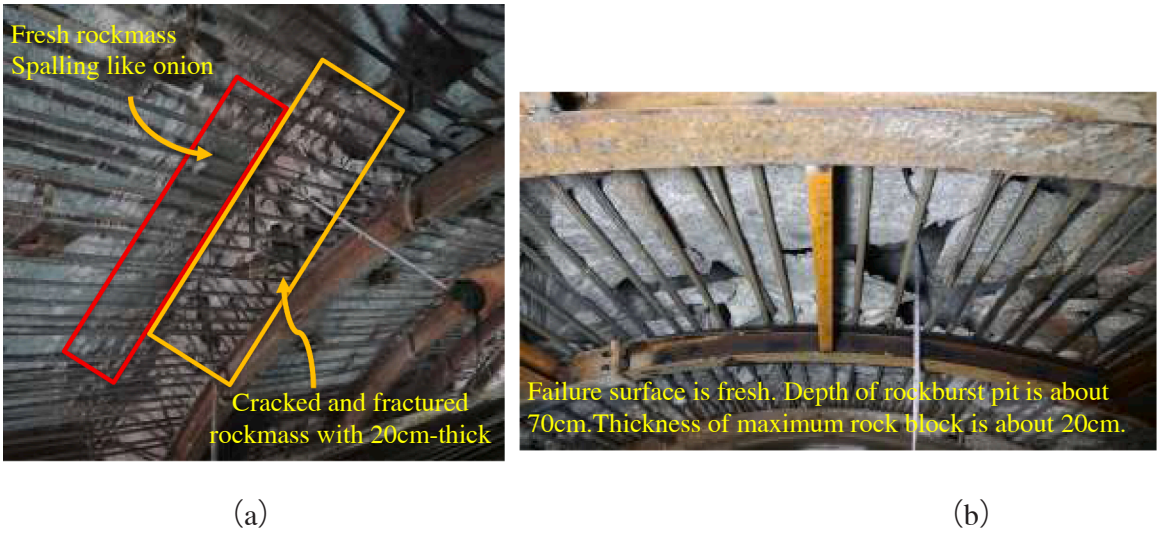

Fig. 17. Slabbing and slight rockburst in the tunnel in Xinjiang Province under high stress. (a) Slabbing in the left vault, (b) Slight rockburst in the upper vault.

in the left vault of the tunnel on November 22 and 23 in Fig. 16, and rock mass spalling can be observed in the left vault of the tunnel in Fig. 17. Few events were triggered in the period between November 24–28, indicating that the rock mass rupture that occurred in these five days was not serious. On November 29 and 30, the rock microcracks moved towards the tunnel's upper vault, and slight rockburst occurred in the tunnel's upper vault. As zones and risks of rock fracture were warned, the supports were strengthened by the H-beam arch frame supporting structures with reinforcement rows in the left and upper vault of the tunnel, and personnel and equipment remained uninjured as spalling and slight rockburst occurred. Therefore, the proposed method is significant in locating the microcrack source and disaster warning in rock engineering.

6. Conclusion

(1) Adverse sensor array and significant data error can lead to ill-conditioned problem in location. The sensor array interferes with the location results by amplifying errors such as arrival time and wave velocity, thereby covering the true solution of the source, ultimately leading to location divergence.

(2) To solve the problem, the ND method is enhanced to equalize the dimensions of source parameters, thereby reducing the condition number of the coefficient matrix and increasing the minimum singular value. Additionally, an improved regularized ND method is introduced based on the regularization process. This method enhances the coefficient matrix and determines the regularization factor using the L-curve to mitigate the singularity of the ill-conditioned equation and convert the ill-conditioned problem into a non-ill-conditioned one.

(3) The residual isosurface of a non-ill-conditioned event presents an ellipsoidal distribution, decreasing with iteration until it eventually shrinks to a point. The residual isosurface of an ill-conditioned event presents a conical distribution, with the vertex of the cone gradually extending into the distance. In the case of ill-conditioned events, the location results of the ND method diverge and cannot converge near the source. However, in the iteration of the improved regularized ND method, the singular value and condition number are controlled, leading to the convergence of the location result. For non-ill-conditioned events, both methods can converge to the optimal position, but the improved regularized ND method increases the computation.

(4) According to the comparison between the ill-conditioned and non-ill-conditioned events, when the minimum singular value σ_4 is less than 1.0×10^{-7} and the condition number is greater than 1.0×10^{7} at the end of the iteration, the events are ill-conditioned and can be located by the improved regularized ND method. Otherwise, the event is non-ill-conditioned and the ND method can be used to solve it quickly. Based on this method, we validated it using data from a diversion tunnel project. Compared to the traditional method, the number of the events obtained by the improved regularized ND method is increased by 194.7 %, the location accuracy and utilization rate of the data are improved significantly. Position of microcracks in cross-section can be recognized by the proposed method, this is crucial for safe construction of tunnelling engineering.

Declaration of Competing Interest

The authors declared that they have no conflicts of interest to this work. We declare that we do not have any commercial or associative interest that represents a conflict of interest in connection with the work submitted.

Acknowledgments

The authors are grateful for the financial support from the National Natural Science Foundation of China (Grant no. 42077263). We would like to thank the staff at the Beiminghe Iron Mine of Minmetals Hanxing Mining Co., Ltd., in Hebei Province and Hubei Seaquake technology Co., Ltd., and teacher Yao Zhibin and Mr. Hao JianJun for their support and assistance in the field monitoring and data analysis.

References

[1] M. Benzi, Preconditioning techniques for large linear systems: a survey, J. Comput. Phys. 182 (2002) 418–477, https://doi.org/10.1006/jcph.2002.7176.
[2] A. Bouhamidi, K. Jbilou, L. Reichel, H. Sadok, An extrapolated TSVD method for linear discrete ill-posed problems with Kronecker structure, Linear Algebra Appl. 434 (2011) 1677–1688, https://doi.org/10.1016/j.laa.2010.06.001.
[3] B., R. Chen, T. Li, X., H. Zhu, X. Wang, M., X. Xie, Microseismic source location method based on a velocity model database and statistical analysis, Arab. J. Geosci. 14 (2021) 1–16, https://doi.org/10.1007/s12517-021-08311-9.
[4] J.L. Cheng, G.D. Song, T.Y. Liu, B.X. Hu, J.Q. Wang, J.Y. Wang, High precision location of micro-seismic sources in underground coal mine, Chin. J. Geophys. -Chin. Ed. 59 (2016) 4513–4520, https://doi.org/10.6038/cjg20161214.
[5] R.S. Crosson, Crustal structure modeling of earthquake data: 1. Simultaneous least-squares estimation of hypocenter and velocity parameters, J. Geophys. Res. 81 (1976) 3036–3046, https://doi.org/10.1029/JB081i017p03036.
[6] L. Eldén, Algorithms for the regularization of ill-conditioned least squares problems, BIT Numer. Math. 17 (1977) 134–145, https://doi.org/10.1007/BF01932285.
[7] G.L. Feng, X.T. Feng, B.R. Chen, Y.X. Xiao, Performance and feasibility analysis of two microseismic location methods used in tunnel engineering, Tunn. Undergr. Space Technol. 63 (2017) 183–193, https://doi.org/10.1016/j.tust.2017.01.006.
[8] L. Geiger, Probability method for determination of earthquake epicenters from arrival time only, Bull. St. Louis Univ. 8 (1912) 60–71.
[9] P., C. Hansen, The discrete picard condition for discrete ill-posed problems, BIT Numer. Math. 30 (1990) 658–672, https://doi.org/10.1007/BF01933214.
[10] P.C. Hansen, Analysis of discrete ill-posed problems by means of the L-Curve, Siam Rev. 34 (1992) 561–580, https://doi.org/10.1137/1034115.
[11] P.C. Hansen, Regularization tools: a Matlab package for analysis and solution of discrete ill-posed problems, Numer. Algorithms 6 (1994) 1–35, https://doi.org/10.1007/BF02149761.
[12] P.C. Hansen, D.P. Oleary, The use of the L-Curve in the regularization of discrete ill-posed problems, Siam J. Sci. Comput. 14 (1993) 1487–1503, https://doi.org/10.1137/0914086.
[13] J.S. Hong, H.S. Lee, D.-H. Lee, H.-T. Kim, Y.T. Choi, Y. Park, Microseismic event monitoring of highly stressed rock mass around underground oil storage caverns, Tunn. Undergr. Space Technol. 21 (2006) 292, https://doi.org/10.1016/J.TUST.2005.12.151.
[14] L. Hu, X.T. Feng, Y.X. Xiao, R. Wang, G.L. Feng, Z.B. Yao, W.J. Niu, W. Zhang, Effects of structural planes on rockburst position with respect to tunnel cross-sections: a case study involving a railway tunnel in China, Bull. Eng. Geol. Environ. 79 (2020) 1061–1081, https://doi.org/10.1007/s10064-019-01593-0.
[15] Y. Jiang, P. Peng, L. Wang, Z. He, Automated locating mining-induced microseismicity without arrival picking by weighted STA/LTA traces stacking, Sustainability 12 (2020) 3665, https://doi.org/10.3390/su12093665.
[16] A. Kijko, An algorithm for the optimum distribution of a regional seismic network-I, Pure Appl. Geophys. 115 (1977) 999–1009, https://doi.org/10.1007/BF00881222.
[17] A. Kijko, An algorithm for the optimum distribution of a regional seismic network-II : an analysis of the accuracy of location of local earthquakes depending on the number of seismic stations, Pure Appl. Geophys. 115 (1977) 1011–1021, https://doi.org/10.1007/BF00881223.
[18] C.Y. Ku, A novel method for solving ill-conditioned systems of linear equations with extreme physical property contrasts, Comput. Model. Eng. Sci. 96 (2013) 409–434, https://doi.org/10.3970/cmes.2013.096.409.
[19] B.F. Li, Y.Z. Shen, Y.M. Feng, Fast GNSS ambiguity resolution as an ill-posed problem, J. Geod. 84 (2010) 683–698, https://doi.org/10.1007/s00190-010-0403-5.
[20] N. Li, M.C. Ge, E.Y. Wang, Two types of multiple solutions for microseismic source location based on arrival-time-difference approach, Nat. Hazards 73 (2014) 829–847, https://doi.org/10.1007/s11069-014-1110-y.
[21] N. Li, E.Y. Wang, M.C. Ge, Z.Y. Sun, A nonlinear microseismic source location method based on Simplex method and its residual analysis, Arab. J. Geosci. 7 (2014) 4477–4486, https://doi.org/10.1007/s12517-013-1121-0.
[22] Q. Li, N. Wang, D. Yi, Numerical Analysis, Tsinghua University Press, 2001.
[23] P.X. Li, B.R. Chen, Y.X. Xiao, G.L. Feng, Y.Y. Zhou, J.S. Zhao, Rockburst and microseismic activity in a lagging tunnel as the spacing between twin TBM excavated tunnels changes: a case from the Neelum-Jhelum hydropower project, Tunn. Undergr. Space Technol. 132 (2023) 104884, https://doi.org/10.1016/j.tust.2022.104884.
[24] Q.P. Li, B.R. Chen, Research on micro-seismic source location during linear excavation process of deep tunnel, in: X.T. Feng, J.A. Husdson (Eds.), Rock. Character, Model. Eng. Des. Methods (2013) 675–680.
[25] T. Li, M.F. Cai, M. Cai, A review of mining-induced seismicity in China, Int. J. Rock. Mech. Min. Sci. 44 (2007) 1149–1171, https://doi.org/10.1016/j.ijrmms.2007.06.002.
[26] X.W. Li, B. Zhou, C.Y. Bai, J.L. Wu, Seismic complex ray tracing in 2D/3D viscoelastic anisotropic media by a modified shortest-path method, Geophysics 85 (2020) T331–T342, https://doi.org/10.1190/geo2020-0113.1.

[27] C.S. Liu, A two-side equilibration method to reduce the condition number of an ill-posed linear system, CMES-Comput. Model. Eng. Sci. 91 (2013) 17–42, https://doi.org/10.3970/CMES.2013.091.017.
[28] C.S. Liu, C.L. Kuo, A dynamical tikhonov regularization method for solving nonlinear ill-posed problems, CMES-Comput. Model. Eng. Sci. 76 (2011) 109–132, https://doi.org/10.3970/CMES.2011.076.109.
[29] C.P. Lu, G.J. Liu, Y. Liu, N. Zhang, J.H. Xue, L. Zhang, Microseismic multi-parameter characteristics of rockburst hazard induced by hard roof fall and high stress concentration, Int. J. Rock. Mech. Min. Sci. 76 (2015) 18–32, https://doi.org/10.1016/j.ijrmms.2015.02.005.
[30] T.H. Ma, C.A. Tang, L.X. Tang, W.D. Zhang, L. Wang, Rockburst characteristics and microseismic monitoring of deep-buried tunnels for Jinping II Hydropower Station, Tunn. Undergr. Space Technol. 49 (2015) 345–368, https://doi.org/10.1016/j.tust.2015.04.016.
[31] N. Maeda, A method for reading and checking phase times in autoprocessing system of seismic wave data, Zisin 38 (2) (1985) 365–379.
[32] A.J. Mendecki, Seismic Monitoring in Mines, Chapman and Hall Press, 1997.
[33] P. Peng, Y. Jiang, L. Wang, Z., X. He, Microseismic event location by considering the influence of the empty area in an excavated tunnel, Sensors 20 (2020) 574, https://doi.org/10.3390/s20020574.
[34] M.J.D. Powell, An efficient method for finding the minimum of a function of several variables without calculating derivatives, Comput. J. 7 (1964) 155–162, https://doi.org/10.1093/COMJNL/7.2.155.
[35] H. Rindorf, Acoustic emission source location in theory and in practice, Tech. Rev. - Bruel Kjaer Engl. Ed. 2 (1981) 3–44.
[36] Y.H. Shi, R. Eberhart, A modified particle swarm optimizer, 1998 IEEE Int. Conf. Evolut. Comput. Proc. (1998) 69–73, https://doi.org/10.1109/ICEC.1998.699146.
[37] C.H. Thurber, Nonlinear earthquake location - theory and examples, Bull. Seismol. Soc. Am. 75 (1985) 779–790, https://doi.org/10.1785/BSSA0750030779.
[38] A.N. Tikhonov, V.Y. Arsenin, Solutions of Ill-posed Problems, WILEY Press, 1977.
[39] J. Um, C. Thurber, A fast algorithm for two-point seismic ray tracing, Bull. Seismol. Soc. Am. 77 (1987) 972–986, https://doi.org/10.1785/BSSA0770030972.
[40] B.F. Vajargah, M. Moradi, Diagonal scaling of Ill-Conditioned Matrixes by Genetic Algorithm, J. Appl. Math., Stat. Inform. 8 (2012) 49–53, https://doi.org/10.2478/v10294-012-0005-3.
[41] N.W. Xu, T.B. Li, F. Dai, B. Li, Y.G. Zhu, D.S. Yang, Microseismic monitoring and stability evaluation for the large scale underground caverns at the Houziyan hydropower station in Southwest China, Eng. Geol. 188 (2015) 48–67, https://doi.org/10.1016/j.enggeo.2015.01.020.
[42] Y.C. Zhang, J. Duchi, M. Wainwright, Divide and conquer kernel ridge regression: A distributed algorithm with minimax optimal rates, J. Mach. Learn. Res. 16 (2015) 3299–3340, https://doi.org/10.48550/arXiv.1305.5029.
[43] J.S. Zhao, Q. Jiang, J.F. Lu, B.R. Chen, S.F. Pei, Z.L. Wang, Rock fracturing observation based on microseismic monitoring and borehole imaging: In situ investigation in a large underground cavern under high geostress, Tunn. Undergr. Space Technol. 126 (2022) 104549, https://doi.org/10.1016/j.tust.2022.104549.
[44] J.S. Zhao, B.R. Chen, Q. Jiang, J.F. Lu, X.J. Hao, S.F. Pei, F. Wang, Microseismic monitoring of rock mass fracture response to blasting excavation of large underground caverns under high geostress, Rock. Mech. Rock. Eng. 55 (2022) 733–750, https://doi.org/10.1007/s00603-021-02709-3.
[45] X.Z. Zhao, B.Y. Ye, Similarity of signal processing effect between Hankel matrix-based SVD and wavelet transform and its mechanism analysis, Mech. Syst. Signal Process. 23 (2009) 1062–1075, https://doi.org/10.1016/j.ymssp.2008.09.009.

Bing-Rui Chen is a Professor of Northeastern University, China. He obtained his B.Sc. and Ph.D. from Northeastern University, China. He is a Vice Chairman of Crustal Stress and Earthquake Committee of Chinese Society of Rock Mechanics and Engineering (CSRME). He is also an Editorial Board Member of *Gold Science and Technology* and Young Editorial Board Member of *Tunnelling Construction*. He won one Second Prize of National Science and Technology Progress Award (Ranking 3), one First Prize of Technological Invention, one Patent Gold Award and one Patent Silver Award in Hubei Province and one Patent Excellence Award in China (Ranking1). His research interests are microseismic monitoring technology, analysis and early warning methods, and protection of rock engineering disasters.